

Research of Novel Three-phase Inverter and its Modulation Technique

Wang Shuwen^{1, 2}, Ji Yanchao¹, Fang Junlong¹

1. Harbin Institute of Technology, Harbin, Heilongjiang 150001, China. Email: wswtr@163.com

2. Northeast agricultural University, Harbin, Heilongjiang 150001, China

Abstract: This paper proposes a novel three-phase uncontrollable rectifier inverter without or with a quite small dc-link capacitor. Because a modulation wave reconstruction-SPWM (MWR-SPWM) technique is adopted which can greatly eliminate the harmonics of output voltage, the DC filter capacitor is greatly decreased or even removed. In addition, the size of the input ac filter and the output ac filter is reduced. The principle of operation and harmonics elimination of the novel inverter topology are elaborated. A through analysis on its performance is presented. This inverter has many advantages such as simpler structure, higher reliability, more effective harmonics elimination. The performance of this inverter using MWR-SPWM technique is compared with traditional inverter by simulation and experiment, and the results show that the theoretical analysis is correct. [Nature and Science. 2006;4(3):28-36].

Keywords: inverter; MWR-SPWM; harmonics elimination

I. INTRODUCTION

Inverter are widely used in many industrial applications such as variable-frequency velocity modulation^{[1][2][3]}, UPS, VAR compensator etc. In order to supply high quality power for loads, it is significant for this inverter to eliminate harmonics in output voltage effectively. Pulse width modulation (PWM) technique that has satisfied performance in harmonics elimination, voltage regulation, responding speed is widely used in all kinds of inverters.^{[4][5]}

Conventionally, all PWM-controlled inverters are based on ideal dc voltage, in practice a bulky dc filter capacitor is installed after the three-phase uncontrollable rectifier to obtain low-ripple dc voltage, as shown in Figure 1. However, the dc filter capacitor has several disadvantages from the viewpoints of size, weight, cost, and reliability^[6]. Moreover, the properties of the dc filter capacitor deteriorate gradually due to continuous

out-gassing. Hence, dc filter capacitor is the major factor limiting the lifetime of inverter systems^[7].

In order to solve the above-mentioned problems, we propose a novel three-phase inverter based on modulation wave reconstruction - SPWM (MWR-SPWM) technique, as shown in Figure 2. Due to MWR-SPWM technique is adopted, the dc filter capacitor is decreased largely or even removed and the harmonics in output voltage is eliminated effectively. The main use of capacitor isn't filtering harmonics but buffering energy. When the power factor of load is high enough, the capacitor can be omitted. Meanwhile the size of input ac filter and the output ac filter are proportionately reduced.

II. PRINCIPLE OF OPERATION

The novel inverter topology mainly consists of a three-phase diode bridge and an inverter. The output of

the three-phase diode bridge rectifier V_{dc} is a type of six-pulse dc voltage as shown in Figure 3, which contains inherent harmonics of the $6n f_0$ (f_0 is the system frequency) besides dc component. Using conventional SPWM technique the output voltage of inverter V_{out} contains harmonics of $f_{6k} \pm f_{sin}$ ($f_{6k} = 6kf_0$, f_{sin} is the modulation wave frequency) besides fundamental component in low frequency band. How can we obtain the desired fundamental component and eliminate the unwanted low-order harmonics in V_{out} by a simple approach?

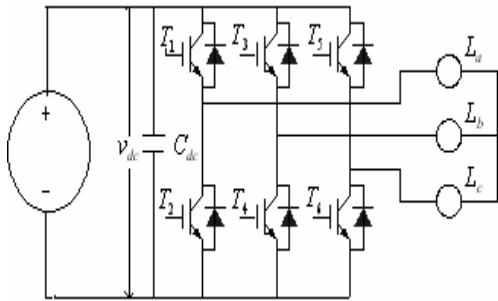


Figure 1. A conventional inverter

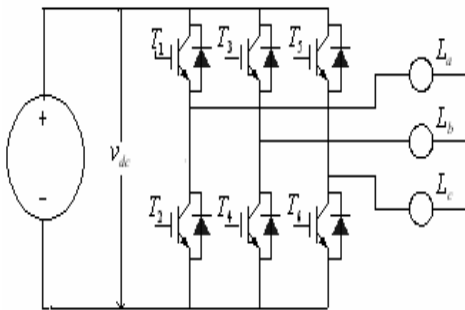


Figure 2. The proposed inverter

We can achieve this purpose by using modulation wave reconstruction-SPWM technique. Meanwhile the value and frequency regulation of the output voltage can be conventionally achieved by regulating modulation wave. In the next section, the detailed analysis is given.

III. MODULATION WAVE RECONSTRUCTION - SPWM TECHNIQUE

1. Analysis of Output Voltage Using Conventional SPWM Technique

In this section, the proposed inverter is analyzed under steady-state condition.

In Figure 2, v_{dc} is the output dc voltage of the three-phase diode bridge rectifier, we choose its midpoint as zero potential reference. In order to make the analysis comprehensive, the expression of v_{dc} can be represented by the following Fourier series in (1).

$$v_{dc} = V_D + \sum_{i=1}^{\infty} U_i \cos \phi_i \cos w_i t + \sum_{i=1}^{\infty} U_i \sin \phi_i \sin w_i t \quad (1)$$

Firstly, we chose standard three-phase sinusoidal wave as modulation wave, take phase a for example, it's expressed as follows.

$$u_{s1} = U_B \sin(\omega t + \theta) \quad (2)$$

Figure 3 shows the relationship among triangular-wave voltage u_{tr} , modulation wave voltage u_{s1} and voltage of a phase u_a . Switching status is determined by the compared result between u_{s1} and u_{tr} as follows: the switch turns on when $u_{s1} > u_{tr}$, but turns off when $u_{s1} < u_{tr}$. The frequency of triangular-wave f_{tr} is M times to the frequency of sinusoidal modulation wave f_{sin} . The sinusoidal wave is "chopped" 2 M times in per sinusoidal cycle. We get 2 M angles, define them as α_i ($i = 1, 2, \dots, 2 M$).

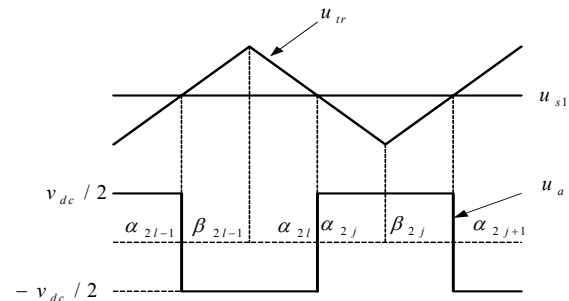


Figure 3. The relationship of u_{tr} , u_{s1} , u_a ,

When (1) is modulated under (2), the Fourier series coefficients of output voltage u_a are respectively expressed as $a_n^{(1,1)}$, $b_n^{(1,1)}$, $a_n^{(2,1)}$, $b_n^{(2,1)}$, $a_n^{(3,1)}$, $b_n^{(3,1)}$. The output voltage u_a fluctuates between $v_{dc}/2$ and $-v_{dc}/2$, and its Fourier series can be expressed as (3), given at the bottom of this page.

Since the frequency of the triangular wave is sufficiently high, we can believe that u_{s1} and v_{dc} is constant during one triangular-wave cycle.

Therefore

$$\frac{\alpha_{2j+1} + \alpha_{2j}}{2} \approx \beta_{2j} \quad (4)$$

$$\frac{\alpha_{2l} + \alpha_{2l-1}}{2} \approx \beta_{2l-1} \quad (5)$$

$$\frac{\alpha_{2j+1} - \alpha_{2j}}{2} \approx \frac{U_B \sin(\beta_{2j} + \theta) - V_{trl}}{V_{trm} - V_{trl}} \cdot \frac{\omega T_{tr}}{2} \quad (6)$$

$$\frac{\alpha_{2l} - \alpha_{2l-1}}{2} \approx \frac{V_{trm} - U_B \sin(\beta_{2l-1} + \theta)}{V_{trm} - V_{trl}} \cdot \frac{\omega T_{tr}}{2} \quad (7)$$

$$\sin\left(n \frac{\alpha_{2j+1} - \alpha_{2j}}{2}\right) \approx n \frac{\alpha_{2j+1} - \alpha_{2j}}{2} \quad (8)$$

$$\sin\left(n \frac{\alpha_{2l} - \alpha_{2l-1}}{2}\right) \approx n \frac{\alpha_{2l} - \alpha_{2l-1}}{2} \quad (9)$$

$a_n^{(1,1)}$ is expressed as (10), given at the bottom of this page. Substituting (4)--(9) into (10), we can obtain (11).

Because ωT_{tr} is so small, we can convert the form of the first step in (11) into an integral one, which simplifies the result. $b_n^{(1,1)}$ can be derived by using the same method.

$$u_a = \frac{1}{2} (a_0^{(1,1)} + a_0^{(2,1)} + a_0^{(3,1)}) + \sum_{n=1}^{\infty} [(a_n^{(1,1)} + a_n^{(2,1)} + a_n^{(3,1)}) \cos n\omega t + (b_n^{(1,1)} + b_n^{(2,1)} + b_n^{(3,1)}) \sin n\omega t] \quad (3)$$

$$a_n^{(1,1)} = \frac{1}{2} \left[\sum_{j=1}^M \frac{1}{\pi} \int_{\alpha_{2j}}^{\alpha_{2j+1}} U_D \cos n\alpha d\alpha + \sum_{l=1}^M \frac{1}{\pi} \int_{\alpha_{2l-1}}^{\alpha_{2l}} (-U_D) \cos n\alpha d\alpha \right] \quad (n=0, 1, 2, \dots) \quad (10)$$

$$= \frac{1}{2} \left[\sum_{j=1}^M \frac{2U_D}{n\pi} \cos\left(n \frac{\alpha_{2j+1} + \alpha_{2j}}{2}\right) \sin\left(n \frac{\alpha_{2j+1} - \alpha_{2j}}{2}\right) + \sum_{l=1}^M \frac{-2U_D}{n\pi} \cos\left(n \frac{\alpha_{2l} + \alpha_{2l-1}}{2}\right) \sin\left(n \frac{\alpha_{2l} - \alpha_{2l-1}}{2}\right) \right]$$

$$\begin{aligned}
 a_n^{(1,1)} &\approx \frac{1}{2} \left[\sum_{j=1}^M \frac{2U_D}{\pi} \cos n\beta_{2j} \frac{U_B \sin(\beta_{2j} + \theta) - V_{trl}}{V_{trm} - V_{trl}} \cdot \frac{\omega T_{tr}}{2} \right. \\
 &\quad \left. + \sum_{l=1}^M -\frac{2U_D}{\pi} \cos n\beta_{2l-1} \frac{V_{trm} - U_B \sin(\beta_{2l-1} + \theta)}{V_{trm} - V_{trl}} \cdot \frac{\omega T_{tr}}{2} \right] \\
 &= \frac{U_D}{2\pi(V_{trm} - V_{trl})} \int_{-\pi}^{\pi} -U_B \sin((n-1)\beta - \theta) d\beta \quad (n = 0, 1, 2, \dots) \quad (11)
 \end{aligned}$$

$$\begin{aligned}
 b_n^{(1,1)} &= \frac{1}{2} \left[\sum_{j=1}^M \frac{1}{\pi} \int_{\alpha_{2j}}^{\alpha_{2j+1}} U_D \sin n\alpha d\alpha \right. \\
 &\quad \left. + \sum_{l=1}^M \frac{1}{\pi} \int_{\alpha_{2l-1}}^{\alpha_{2l}} (-U_D) \sin n\alpha d\alpha \right] = \frac{U_D}{2\pi(V_{trm} - V_{trl})} \int_{-\pi}^{\pi} U_B \cos((n-1)\beta - \theta) d\beta \quad (12)
 \end{aligned}$$

$a_n^{(2,1)}$ can be expressed as (13). Substituting (4)—(9) into (13), we can obtain (14).

$$\begin{aligned}
 a_n^{(2,1)} &= \frac{1}{2} \left[\sum_{j=1}^M \frac{1}{\pi} \int_{\alpha_{2j}}^{\alpha_{2j+1}} \sum_{k=1}^{\infty} U_k \cos \phi_k \cos(\omega_k \pm n) \frac{\alpha_{2j+1} + \alpha_{2j}}{2} \cos n\alpha d\alpha \right. \\
 &\quad \left. + \sum_{l=1}^M \frac{1}{\pi} \int_{\alpha_{2l-1}}^{\alpha_{2l}} \sum_{k=1}^{\infty} -U_k \cos \phi_k \cos(\omega_k \pm n) \frac{\alpha_{2j+1} + \alpha_{2j}}{2} \cos n\alpha d\alpha \right] \\
 &= \frac{1}{2\pi} \left\{ \sum_{j=1}^M \left[\sum_{k=1}^{\infty} \frac{1}{\frac{\omega_k}{\omega} \pm n} U_k \cos \phi_k \cos\left(\frac{\omega_k}{\omega} \pm n\right) \frac{\alpha_{2l+1} + \alpha_{2l}}{2} \cdot \sin\left(\frac{\omega_k}{\omega} \pm n\right) \frac{\alpha_{2l+1} - \alpha_{2l}}{2} \right] \right. \\
 &\quad \left. - \sum_{l=1}^M \left[\sum_{k=1}^{\infty} \frac{1}{\frac{\omega_k}{\omega} \pm n} U_k \cos \phi_k \cos\left(\frac{\omega_k}{\omega} \pm n\right) \frac{\alpha_{2l+1} + \alpha_{2l}}{2} \cdot \sin\left(\frac{\omega_k}{\omega} \pm n\right) \frac{\alpha_{2l+1} - \alpha_{2l}}{2} \right] \right\} \quad (13)
 \end{aligned}$$

$$\begin{aligned}
 a_n^{(2,1)} &\approx \frac{1}{2\pi} \left\{ \sum_{j=1}^M \sum_{k=1}^{\infty} \left[\left(\cos\left(\frac{\omega_k}{\omega} + n\right) \beta_{2j} \frac{U_B \sin(\beta_{2j} + \theta) - V_{trl}}{V_{irm} - V_{trl}} \right) \right. \right. \\
 &\quad \left. \left. + \cos\left(\frac{\omega_k}{\omega} - n\right) \beta_{2j} \frac{U_B \sin(\beta_{2j} + \theta) - V_{trl}}{V_{irm} - V_{trl}} \right) \cdot \frac{\omega T_{tr}}{2} \cdot U_k \cos \phi_k \right] \\
 &\quad - \sum_{l=1}^M \sum_{k=1}^{\infty} \left[\left(\cos\left(\frac{\omega_k}{\omega} + n\right) \beta_{2j} \frac{V_{irm} - U_B \sin(\beta_{2l-1} + \theta)}{V_{irm} - V_{trl}} \right) \right. \\
 &\quad \left. + \cos\left(\frac{\omega_k}{\omega} - n\right) \beta_{2j} \frac{V_{irm} - U_B \sin(\beta_{2l-1} + \theta)}{V_{irm} - V_{trl}} \right) \cdot \frac{\omega T_{tr}}{2} U_k \cos \phi_k \right] \\
 &= \frac{\omega T_{tr}}{2\pi(V_{irm} - V_{trl})} \left\{ \sum_{j=1}^M \sum_{k=1}^{\infty} \left[\left(\frac{U_B}{2} \begin{pmatrix} \sin\left(\left(6k \frac{\omega_k}{\omega} + 1 \pm n\right) \beta_{2j} + \theta\right) \\ -\sin\left(\left(6k \frac{\omega_k}{\omega} - 1 \pm n\right) \beta_{2j} - \theta\right) \end{pmatrix} \right) \right. \right. \\
 &\quad \left. \left. - \cos\left(\frac{\omega_k}{\omega} \pm n\right) \beta_{2j} V_{trl} \right) \cdot U_k \cos \phi_k \right] \\
 &\quad - \sum_{l=1}^M \sum_{k=1}^{\infty} \left[\left(-\frac{U_B}{2} \begin{pmatrix} \sin\left(\left(\frac{\omega_k}{\omega} + 1 \pm n\right) \beta_{2l-1} + \theta\right) \\ -\sin\left(\left(\frac{\omega_k}{\omega} - 1 \pm n\right) \beta_{2l-1} - \theta\right) \end{pmatrix} \right) \right. \\
 &\quad \left. \left. + \cos\left(\frac{\omega_k}{\omega} \pm n\right) \beta_{2l-1} V_{irm} \right) \cdot U_k \cos \phi_k \right] \right\} \quad (14)
 \end{aligned}$$

Because the frequency of triangular-wave is sufficiently high, we can believe that

$\sin\left(\left(\frac{\omega_k}{\omega} + 1 \pm n\right) \alpha + \theta\right)$ is constant during one

triangular-wave cycle. Therefore, we can obtain (15) and (16), which are shown at the bottom of this page.

$$\sum_{j=1}^M \sin\left(\left(\frac{\omega_k}{\omega} + 1 \pm n\right) \beta_{2j} + \theta\right) \cdot \omega T_{tr} \approx \int_{-\pi}^{\pi} \sin\left(\left(\frac{\omega_k}{\omega} + 1 \pm n\right) + \theta\right) d\beta \quad (15)$$

$$\sum_{l=1}^M \sin\left(\left(\frac{\omega_k}{\omega} + 1 \pm n\right) \beta_{2l-1} + \theta\right) \cdot \omega T_{tr} \approx \int_{-\pi}^{\pi} \sin\left(\left(\frac{\omega_k}{\omega} + 1 \pm n\right) + \theta\right) d\beta \quad (16)$$

Substituting (15), (16) into (14), we can get (17), given at the bottom of this page.

Similarly, $b^{(2,1)}$ can be expressed as (18). By using the same method, we can obtain $a_n^{(3,1)}$ and $b_n^{(3,1)}$, shown in (19) and (20) respectively.

$$a_n^{(2,1)} \approx \frac{1}{4\pi(V_{trm} - V_{trl})} \sum_{k=1}^{\infty} U_k \cos \phi_k \cdot \int_{-\pi}^{\pi} \left[\begin{array}{l} U_B \sin \left[\left(\frac{\omega_k}{\omega} - n + 1 \right) \beta + \theta \right] \\ + U_B \sin \left[\left(\frac{\omega_k}{\omega} - n - 1 \right) \beta - \theta \right] \\ - (V_{trm} + V_{trl}) \cos \left(\frac{\omega_k}{\omega} - n \right) \beta \end{array} \right] d\beta \quad (17)$$

$$b_n^{(2,1)} = \frac{1}{2} \left[\begin{array}{l} \sum_{j=1}^M \frac{1}{\pi} \int_{\alpha_{2j}}^{\alpha_{2j+1}} \sum_{k=1}^{\infty} U_k \cos \phi_k \cos(\omega_k \pm n) \frac{\alpha_{2j+1} + \alpha_{2j}}{2} \sin n \alpha d\alpha \\ + \sum_{l=1}^M \frac{1}{\pi} \int_{\alpha_{2l-1}}^{\alpha_{2l}} \sum_{k=1}^{\infty} -U_k \cos \phi_k \cos(\omega_k \pm n) \frac{\alpha_{2j+1} + \alpha_{2j}}{2} \sin n \alpha d\alpha \end{array} \right]$$

$$= \frac{1}{4\pi(V_{trm} - V_{trl})} \sum_{k=1}^{\infty} U_k \cos \phi_k \int_{-\pi}^{\pi} \left[\begin{array}{l} U_B \cos \left(\left(\frac{\omega_k}{\omega} + 1 - n \right) \beta + \theta \right) \\ - U_B \cos \left(\left(\frac{\omega_k}{\omega} - 1 - n \right) \beta - \theta \right) \\ + \sin \left(\frac{\omega_k}{\omega} - n \right) \beta (V_{trm} + V_{trl}) \end{array} \right] d\beta \quad (18)$$

$$a_n^{(3,1)} = \frac{1}{4\pi(V_{trm} - V_{trl})} \sum_{i=1}^{\infty} U_k \sin \phi_k \int_{-\pi}^{\pi} \left[\begin{array}{l} -U_B \cos \left(\left(\frac{\omega_k}{\omega} - n + 1 \right) \beta + \theta \right) \\ + U_B \cos \left(\left(\frac{\omega_k}{\omega} - n - 1 \right) \beta - \theta \right) \\ - \sin \left(\frac{\omega_k}{\omega} - n \right) \beta (V_{trm} + V_{trl}) \end{array} \right] d\beta \quad (19)$$

$$b_n^{(3,1)} = \frac{1}{4\pi(V_{trm} - V_{trl})} \sum_{k=1}^{\infty} U_k \sin \phi_k \int_{-\pi}^{\pi} \left[\begin{array}{l} U_B \sin \left(\left(\frac{\omega_i}{\omega} + 1 - n \right) \beta + \theta \right) \\ - U_B \sin \left(\left(\frac{\omega_i}{\omega} - 1 - n \right) \beta - \theta \right) \\ - \cos \left(\frac{\omega_i}{\omega} - n \right) \beta (V_{trm} + V_{trl}) \end{array} \right] d\beta \quad (20)$$

$$u_a = \frac{U_D U_B \sin(\omega t + \theta)}{V_{trm} - V_{trl}} + \frac{1}{2} \sum_{k=1}^{\infty} \left(\frac{U_k U_B (\sin((\omega_k + \omega)t + \theta - \phi_k) - \sin((\omega_k - \omega)t - \theta - \phi_k))}{V_{trm} - V_{trl}} \right)$$

$$= \frac{U_D U_B \sin(\omega t + \theta)}{V_{trm} - V_{trl}} + \sum_{k=1}^{\infty} \left(\frac{U_k \cos(\omega_k t - \phi_k) U_B \sin(\omega t + \theta)}{V_{trm} - V_{trl}} \right)$$

$$= \frac{U_D U_B \sin(\omega t + \theta)}{V_{trm} - V_{trl}} + \sum_{k=1}^{\infty} \frac{U_k U_B [\sin(\omega_k t + \omega t - \phi_k + \theta) - \sin(\omega_k t - \omega t - \phi_k - \theta)]}{2(V_{trm} - V_{trl})} \quad (21)$$

Substituting (11), (12), (17), (18), (19), (20) into (3), we can obtain (21). Obviously, u_a contains of a fundamental component, lower harmonics of $f_k \pm f_{sin}$ ($k = 1, 2, \dots, f_k = \omega_k / 2\pi, f_{sin} = \omega / 2\pi$), and harmonics above the switching frequency generated by triangular-wave SPWM operation. Then there is a relationship between u_a and v_{dc} which is expressed as follows:

$$u_a = T(\theta) \cdot v_{dc} \quad (22)$$

Where $T(\theta)$ is the switching function of triggering pulses. Substituting the second step in (21) into (22), we can get the following:

$$T(\theta) = \frac{U_B \sin(\omega t + \theta)}{V_{trm} - V_{trl}} \quad (23)$$

2. Analysis of Output Voltage Using MWR-SPWM Technique

From above analysis, we can add some component to standard modulation wave to offset the influence on output ac

$$u_a = (T'(\theta) + T''(\theta)) \cdot (U_D + \sum_{k=1}^{\infty} U_k \cos(\omega_k t - \phi_k)) = T'(\theta) \cdot U_D \quad (26)$$

$$T''(\theta) = -\frac{\sum_{k=1}^{\infty} U_k \cos(\omega_k t - \phi_k)}{U_D + \sum_{k=1}^{\infty} U_k \cos(\omega_k t - \phi_k)} \cdot T'(\theta) = -\frac{v_{dc} - U_D}{v_{dc}} T'(\theta) \quad (27)$$

Substituting (23) into (27), we obtain the following:

$$T''(\theta) = -\frac{v_{dc} - U_D}{v_{dc}} \cdot \frac{U_B \sin(\omega t + \theta)}{V_{trm} - V_{trl}} \quad (28)$$

When $T''(\theta)$ is compared with $T'(\theta)$, k can be

voltage from dc voltage's fluctuation. Based on this idea, we propose a new modulation wave as follows:

$$u_s = k + u_{s1} \quad (24)$$

We consider that u_s consists of two independent parts, one is u_{s1} , another is k . When (24) is chosen as modulation wave, the switching function $T(\theta)$ can be expressed as follows:

$$T(\theta) = T'(\theta) + T''(\theta) \quad (25)$$

Where $T'(\theta)$ is the component of switching function when modulation wave is u_{s1} which is shown in (23); $T''(\theta)$ is the component of switching function when modulation wave is k .

When the new modulation wave is adopted we hope that the harmonics of u_a can be eliminated effectively, we can obtain (26), given at the bottom of this page. Therefore, we can obtain (27).

obtained by homogeneity theorem.

Therefore, when the new modulation wave u_s is adopted u_a only contains fundamental component in low frequency band.

So, when power system is balanced system, new

modulation wave u_s is adopted that can eliminate the influence of $6nf_0$ harmonics from three-phase diode

$$k = -\frac{v_{dc} - U_D}{v_{dc}} u_{s1} \quad (29)$$

$$u_a \approx \frac{U_D U_B \sin(\omega t + \theta)}{V_{trm} - V_{trl}} \quad (30)$$

IV. SIMULINK AND EXPERIMENTAL RESULT

In order to verify the analyses and the simulation results, a 2-kVA experimental novel inverter that adopts above proposed topology was set up in laboratory. The diode bridge rectifier is connected with a three-phase unbalanced supply. The circuit parameters used in experiment is the same with the ones in simulation.

Figure 4 and Figure 5 show the load phase current waveforms with general SPWM and MWR-SPWM technique respectively. Figure 6 and Figure 7 show the

bridge output voltage to harmonics of converter output voltage so as to not use bulky dc filter capacitor.

output voltage spectrum by using general SPWM and MWR-SPWM technique respectively. Obviously, the novel ac/dc/ac converter can eliminate harmonics of output voltage effectively. The experimental results are in full agreement with theoretical analyses and simulation results.

V. CONCLUSIONS

The proposed novel inverter has such advantages as simpler structure, higher reliability, and higher performance. Moreover, because an MWR-SPWM technique is adopted to eliminate low harmonics in output voltage, not only the bulky dc filter capacitor is greatly decreased or even removed, but also the size of output filter is reduced accordingly. The simulation and experimental results prove the validity of the analysis and the feasibility of the proposed MWR-SPWM technique.

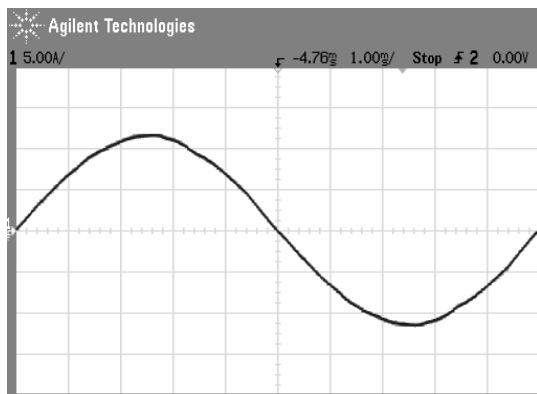


Figure 4. Current waveform using general SPWM technique

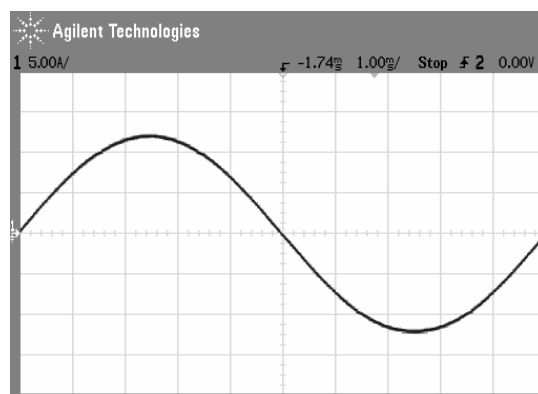


Figure 5. Current waveform by using MWR-SPWM technique

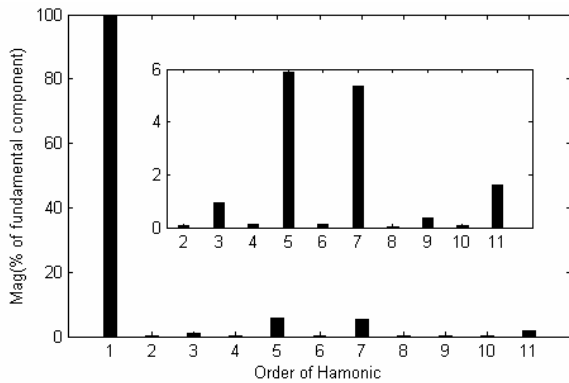


Figure 6. The spectrum of using general SPWM technique

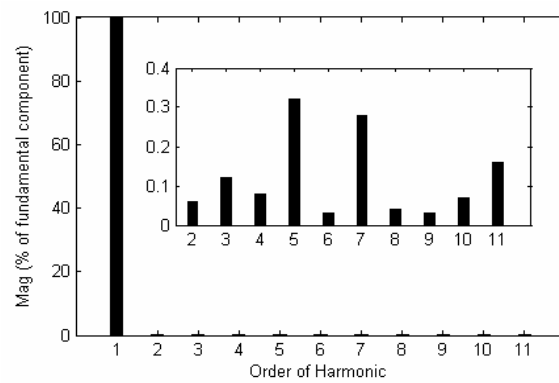


Figure 7. The spectrum of using MWR-SPWM technique

Correspondence to:

Wang Shuwen, Fang Junlong
 Harbin Institute of Technology
 Harbin, Heilongjiang 150001, China
 Email: wswtr@163.com

Information of Authors:

- Wang Shuwen** (1975-) male. He is presently studying at Harbin Institute of Technology for his PhD. In 2002, he joined the Department of Electrical Engineering at NEAU. His research interests include PWM technique, harmonic suppression, and static var compensators.
- Ji Yanchao** (1962-) male. He has been a full-time professor of Electric Engineering at Harbin Institute, since 1993. His research fields include FACTS, static var generators, and generalized active filters.

REFERENCES

- Habetler T G A space vector-based Rectifier Regulator for AC/DC/AC Converters [J]. IEEE Trans. On Power Electronics, 1999,8(1):30~36.

- Hur Namho, Jung Junhwan, Nam Kwanghee. Fast Dynamic DC-link Power balancing Scheme for a PWM converter-inverter System[A]. IECON' 99 Proceedings[C]. The 25th Annual conference of the IEEE, 1999, 2:767~772
- Jung Jinhwan, Lim Sunkyoung, Nam Kwanghee. A Feed-back Linearizing Control Scheme for a PWM Converter –inverter Having a very Small DC-link Capacitor[J].IEEE Trans. on Ind. Appl., 1999,35(5):1124~1131
- Li Li, D. Czarkowski, Yaguang Liu and P. Pillay, “Multilevel selective harmonic elimination PWM technique in series-connected voltage inverters,” IEEE Trans. Ind. Applicat., vol. 36, pp. 160-170, Jan/Feb. 2000.
- Toshiji Kato, “Sequential homotopy-based computation of multiple solutions for selected harmonic elimination in PWM inverters,” IEEE Trans. Cir. and Sys.—I: Fundamental Theory and Application, vol. 46 pp. 586-593, May.1999.
- L. M. Malesani, L. Rossetto, P. Tenti, and P. Tomasin, “AC/DC/AC PWM converter with reduced energy storage in the DC link,” IEEE Trans. Ind. Applicat., vol.31, pp. 287-292, Mar/Apr.1995.
- N. Hur, Jinhwan Jung, Kwanghee Nam, “A fast dynamic DC-link power-balancing scheme for a PWM converter-inverter system,” IEEE Trans. Ind. Applicat., vol. 48, pp. 794-803, Aug.2001.